Biophysical Chemistry 11 (1980) 173–181

TIME DIFFERENCE SCANNING GEL CHROMATOGRAPHY: COMPUTER SIMULATIONS

James K. ZIMMERMAN
Department of Biochemistry, Clemson University, Clemson, SC 29631, USA

Received 16 July 1979; revised manuscript received 4 October 1979

The time difference profile method of gel scanning chromatography developed by Brumbaugh, Saffen and Chun (Biophysical Chemistry, 1979) has been examined by computer simulation. The method is found to produce values for centroid movements that mimic those of the system being examined but are not quantitatively correct. In all cases the time differential "centroid" is larger than that of the concentration derivative (true) centroid and move at a rate slightly faster than the true centroids. This faster rate slowly decreases towards the true rate but does not approach it within reasonable times. This distorted movement reflects the distorted emphasis given to the larger species in the time differential method. The time difference method has been shown to give an adequate measure of the axial dispersion coefficient, L, for single species systems.

1. Introduction

The scanning gel chromatograph developed by Ackers [1] is a powerful and multifunctional instrument [2–9] (For the most recent review see ref. [10]). Recently a time difference technique has been introduced by Brumbaugh, Saffen, and Chun [11,12] where successive scans are subtracted from one another to yield a time difference boundary. These authors desire information concerning partition cross-sections, ξ; partition coefficients, σ; hydrodynamic radii; and other physical parameters. The difference technique has also been applied to systems undergoing self association [12,13]. This paper deals with computer simulations of the difference technique as it is applied to self-associating systems in order to verify or discount the usefulness of these new analytical techniques. In these systems all the parameters are calculated from "ideal" (simulated) profiles and thus can be related to "correct" (input) parameters without the interference of experimental noise.

2. Methods

Computations were performed on an IBM 370/168 digital computer with virtual storage. All graphs in this paper have been produced directly from the computer's Calcomp system. The simulation program used was that described previously [14,15] and is a modification of a program of Cox [16–19]. Briefly this program uses finite difference techniques to solve the basic transport equation of gel chromatography

$$J' = FC'/\xi A - L\,\mathrm{d}C'/\mathrm{d}x \qquad (1)$$

where J' is the solute flux, $(\mathrm{d}m/\mathrm{d}t)/A\xi$, F is the flow rate, A the cross-sectional area, x the distance coordinate, C' the apparent concentration ($C' = C\xi$) [10, 20,21], and ξ is the partition cross-section [14]. The dimensionless parameter, ξ, reflects the relative contribution of the void and internal volumes through the dimensionless parameters α and β [14]

$$\xi = \alpha + \beta\sigma, \qquad (2)$$

where α is the fraction of the volume due to the void volume, β is the fraction of the volume due to the internal volume, and σ is the partition coefficient of the macromolecule. For an associating system, the ap-

Table 1
Equilibrium constants and degree of association

Monomer–n-mer system	Percentage n-mer by weight	K	
		$(mg/ml)^{-(n-1)}$	$M^{-(n-1)}$
Monomer–tetramer			
1	10	1.52×10^{2}	1.87×10^{14}
2	50	8.00×10^{3}	9.83×10^{15}
3	90	9.00×10^{6}	1.11×10^{19}
Monomer–octamer			
1	10	2.32×10^{6}	1.19×10^{35}
2	50	1.28×10^{9}	6.57×10^{37}
3	90	9.00×10^{14}	4.62×10^{43}

propriate parameters are σ_w, the weight average partition coefficient; $F/\xi A$, the weight average velocity; and $\bar{L}$, the gradient average axial dispersion coefficient.

Parameters used in this simulation were similar to those used previously [14] and are listed in tables 1 and 2. In all cases, the system simulated represents column parameters for a Sephadex G-200R column where $\alpha = 0.295$, $\beta = 0.670$, and $F = 1.2$ ml/hr. Direct time profiles were run for a simulated time of 180 minutes; time difference profiles for 180 minutes were obtained either by taking the difference of 200 minute profiles from 160 minute profiles (the mathematics were performed in this order to give positive differences and allow more direct comparisons with derivatives of the direct profiles) or by subtracting a 185 minute profile from a 175 minute profile. All simulations are for the trailing boundary of a large zone experiment [10,20,21].

3. Results and discussion

Fig. 1 shows the results of direct comparisons of the derivatives of directly determined boundaries for six widely differing systems and corresponding time difference profiles. In particular figs. 1D–F, showing a monomer–octamer system, give the most stringent test of the time difference technique's ability to mimic the information present in direct profiles. Figs. 1A–C show a more common situation, that of a monomer–tetramer equilibrium. For both the tetrameric and octameric systems, simulations are shown for systems originally containing 90%, 50%, and 10% monomer. As can be seen, the positions of the peaks of each component visually compare quite nicely, but, not surprisingly, the relative heights and widths do not. In fact, the good correspondence of the heights for the time difference and the derivative curves is strictly coincidental since the heights are completely dependent upon the times chosen for the time differences. This can be seen when comparing a 40 minute difference (fig. 1F) and a 10 minute difference (fig. 2) for the same experimental system. The relative features of the two profiles are maintained but the relative heights are a function of the movement achieved during the time difference. The important difference between

Table 2
System parameters for gel chromatography simulation

Component	Partition coefficient	Axial dispersion coefficient (cm^2/min)	Molecular radius (A)	Molecular weight
Monomer	0.714	3.61×10^{-4}	18.9	17 000
Tetramer	0.474	4.86×10^{-4}	30.0	68 000
Octamer	0.366	7.10×10^{-4}	37.8	136 000

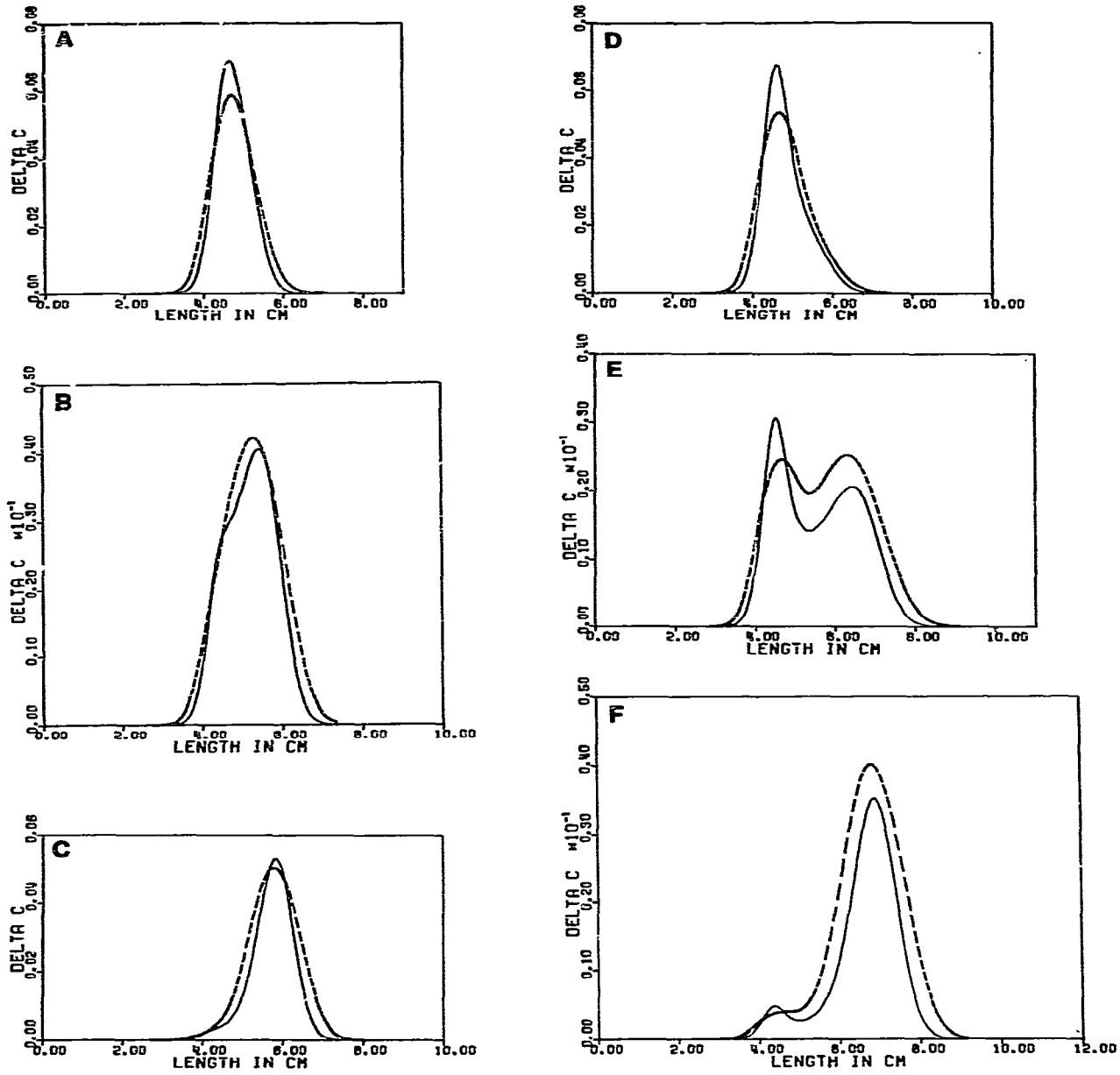

Fig. 1. Comparisons of the derivatives of direct concentration profiles, (dC_T/dx, solid lines), after 180 min of simulation and time difference profiles for time 160–200 min ($C_{(x)t_1} - C_{(x)t_2}$, dotted lines). Time differences are given in this order to make the resulting differences in the trailing edge have a positive value. A. monomer–tetramer; 10% tetramer B. monomer–tetramer; 50% tetramer C. monomer–tetramer; 90% tetramer D. monomer–octamer; 10% octamer E. monomer–octamer; 50% octamer F. monomer–octamer; 90% octamer. Detailed parameters for the simulations are given in the text.

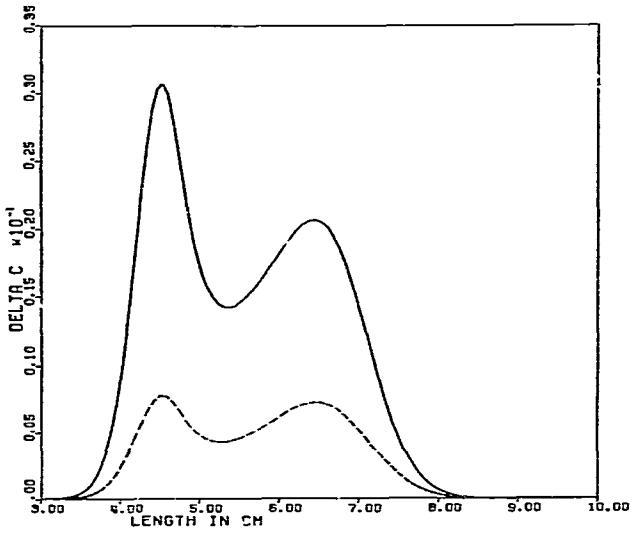

Fig. 2. Comparison of the derivatives of a direct concentration profile (solid line) and a narrow time difference curve (dotted line). Both curves represent the monomer–octamer system with initially 50% octamer. The solid curve is the same as the solid line in fig. 1E but the time difference curve is for a ten minute difference only (175–185 min).

the concentration derivative curves and the time difference curves, however, is the failure of the time difference technique to adequately reflect the relative proportions of the leading and trailing components.

The difference in the relative proportions seen in the graphs is also found when one attempts to calculate the position of the center of mass. When the concentration derivative curves are examined, the correct centroid positions are calculated; however, when the centroids of the time difference profiles are calculated, the resulting values are always greater than the correct value (table 3) reflecting an apparently greater contribution from the larger component than is actually present. These differences are small however, except for the case of the 50% octamer system where the relative proportions of the two concentration derivative peaks are more nearly equal. In an experimental system, with experimental noise, only this one system would show a significant difference from the correct value. While the time difference method is consistently incorrect in obtaining centroid positions, the data of interest are the rates at which successive "centroids" move. In table 4 is shown how the time "centroids" move for two of the simulated systems. The case of the 50% octamer system has been shown to be the worst case of those presented (table 3). Notice that the differences between calculated and real centroids increases as the time increases and also notice that even in this worst case example, the movement of the calculated "centroid" is almost constant, and therefore experimentally no curvature would be detectable. The movement is also somewhat faster than the true rate of movement. This would result in calculated values of ξ, the partition cross-section, and σ, the partition coefficient, being lower than the true values. This also holds for a system where the difference of true and calculated values is not so severe (90% octamer). The rate of movement of the time differential centroids decreases slightly with time but does not approach the correct value even at very long times.

Table 3
Comparison "centroid" positions from differences and concentration differentials

System	True centroid (cm)	Centroid from time difference (cm)	Centroid from concentration derivative (cm)
10% tetramer	4.7536	4.7760	4.7536
50% tetramer	5.1950	5.2455	5.1950
90% tetramer	5.7265	5.7578	5.7265
10% octamer	4.8139	4.8511	4.8131
50% octamer (wide)	5.5664	5.7187	5.5614
50% octamer (narrow)	5.5664	5.7171	5.5664
90% octamer	6.6001	6.6842	6.6001
100% monomer (wide)	4.6549	4.6680	4.6549
100% monomer (narrow)	4.6549	4.6688	4.6549

Table 4
Comparison of "centroid" positions as a function of time

Time (min)	50% Octamer, wide time derivative				90% Octamer			
	True centroid (cm)	Movement of centroid ($\Delta\bar{x}$, cm)	Centroid from time difference (cm)	Movement of time difference centroid ($\Delta\bar{x}$, cm)	True centroid (cm)	Movement of centroid ($\Delta\bar{x}$, cm)	Centroid from time difference (cm)	Movement of time difference centroid ($\Delta\bar{x}$, cm)
60	1.8555	–	1.9286	–	2.2000	–	2.2426	–
90	3.0924	1.2370	3.1929	1.2643	3.6667	1.4667	3.7249	1.4823
140	4.3294	1.2370	4.4563	1.2634	5.1334	1.4667	5.2052	1.4803
180	5.5664	1.2370	5.7187	1.2624	6.6001	1.4667	6.6842	1.4790

Another use for the time difference technique claimed by Brumbaugh et al. [12] is that one can directly calculate values of the axial dispersion coefficient, L. Since this is valid only when a single species is present, simulations were run using the monomer only (fig. 3). These time difference profiles were then analyzed by eq. (9) of Brumbaugh et al. [12] as corrected by Chun (personal communication). However

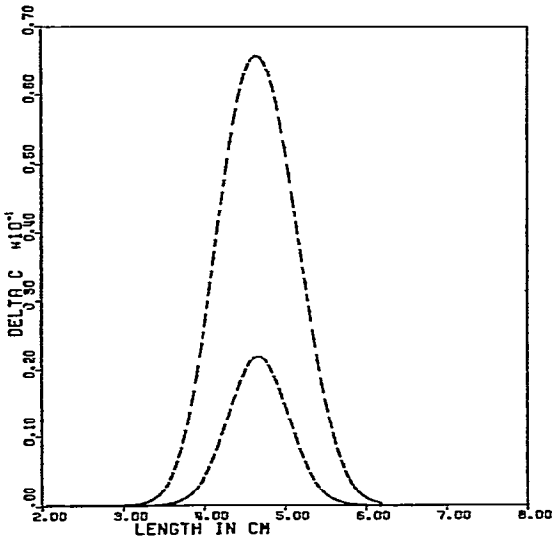

Fig. 3. Comparison of a wide time difference curve (40 min) and a narrower time difference curve (10 min) for a single species. The upper curve is for the difference profile of 160–200 min for the monomer only. The lower curve represents a ten minute difference (175–185 min) for the same system.

those equations lost a factor of two during integration. Also the value of C_0 used by Chun in his discussion is the value of the starting concentration of the bulk solution while the scanner measures an apparent concentration ($C_0' = C_0\xi$). Making these changes, the final equation for L is (see Appendix for derivation and assumptions)

$$L = l^2/2C_0'\Delta t\bar{x}, \tag{3}$$

where

$$l^2 = \int_{-\infty}^{\infty} \frac{C_0'\Delta tF}{\xi\sqrt{4\pi Lt}}(\bar{x} - x)^2 \exp[-(\bar{x} - x)^2/4Lt]\,dx. \tag{4}$$

Because of the way the expression within l^2 is derived and because both l^2 and $\bar{x}$ are functions of time it might be well to ask whether it should be the time of the first profile, the time of the second concentration profile, or the average time that should be used in these calculations; Chun advocates the use of the time of the second concentration profile (personal communication). Table 5 presents these values calculated for all three cases for both the wide and narrow time differences.

Since the generated profiles are not subject to experimental error, one can now compare the calculated value of L with the input value of L (3.61×10^{-4} cm^2/min). As can be seen in table 5, the best values are obtained when t, and the corresponding $\bar{x}$, is the average of the two times scanned. This is not surprising since in that way the $\bar{x} - x$ terms are minimized in the time difference profile. It also can be seen that all of the narrow time calculations come reasonably close .

Table 5
Calculation of dispersion coefficients for the monomer

Simulation	Time (min)	$\bar{x}$ (cm)	l^2 (g)	Calculated L (cm^2/min)	Input L (cm^2/min)
Wide dif. (time 1)	160	4.1377	0.0399	1.56×10^{-3}	3.61×10^{-4}
(avg)	180	4.6549	0.0174	6.04×10^{-4}	3.61×10^{-4}
(time 2)	200	5.1721	0.0377	1.17×10^{-3}	3.61×10^{-4}
Narrow dif. (time 1)	175	4.5256	0.0031	4.44×10^{-4}	3.61×10^{-4}
(avg)	180	4.6549	0.0027	3.75×10^{-4}	3.61×10^{-4}
(time 2)	185	4.7842	0.0030	4.01×10^{-4}	3.61×10^{-4}

to the input value while only the "average time" calculations hold for the wide time difference. Eq. (3), if it were exact, would not have this dependence on Δt. However eq. (3) was developed by looking at the time differential at each x, (dc/dt). Later dc/dt is approximated as $\Delta c/\Delta t$ and therefore the exactness is lost. The smaller the value of Δt, the more exact eq. (3) becomes. This type of determination can only be made on single-species systems since multicomponent systems give curves that are much broader than the gradient average dispersion coefficient would predict, just as the well known case with diffusion coefficients in ultracentrifuge patterns.

4. Summary

The time difference technique of Brumbaugh et al. [12] (also Zimmerman and Grothusen, unpublished observations) has proven itself to be a very valuable tool for increasing the experimental sensitivity of scanning gel chromatography and also for the early detection of components present as a small fraction of the major component. This paper has shown that attempting to absolutely quantitate the movement of a multicomponent system using centroid positions of the difference curve is unjustified (this holds for the movement of single species as well). Each concentration profile itself can be described using an error function complement [10,20,21], and for a single species, the concentration derivatives will describe a gaussian curve in x at any given time. However the difference in two profiles obtained at differing times includes the variable of time and results in a non-gaussian difference profile. This change in variable also explains the fact that centroids cannot quantitatively be obtained by the time difference profile. However, as discussed previously, within experimental error and if looked at with some scepticism, the values of ξ and σ obtained should be reasonably accurate.

This is also the case with the determination of the axial dispersion coefficient, L, at least for monodisperse systems. Computer simulations provide the only adequate test for any derived expressions since currently only one group, other than Chun's, has determined values for L and thus there has not been a great deal of cross-checking using different methods.

From a practical, experimental, point-of-view, the method of time difference profiles appears to be quite useful.

Acknowledgements

The authors would like to thank Dr. P. Chun for the opportunity to examine some of his manuscripts before publication.

Appendix

For a single species, the trailing edge can be described by

$$C_{(x,t)} = \tfrac{1}{2} C_0 \operatorname{erfc} \phi/\sqrt{4Lt}$$

where

$$\operatorname{erfc}(z) = \frac{2}{\sqrt{\pi}} \int_z^\infty e^{-t^2} dt = 1 - \frac{2}{\sqrt{\pi}} \int_0^z e^{-t^2} dt$$

and $\phi = \bar{x} - x$, so that $d\phi = -dx$.

$$C_{(x,t)} = \frac{C_0}{2}\left[\frac{-2}{\sqrt{4\pi L t}} \int_z^\infty \exp[-(\bar{x} - x)^2/4Lt]\, dx\right] = \frac{C_0}{2}\left[\frac{-2}{\sqrt{4\pi L t}} \int_z^\infty \exp(-\phi^2/4Lt)\, d\phi\right]$$

at a constant value of x

$$\frac{dC}{dt} = \frac{-C_0}{\sqrt{4\pi L}}\left\{\frac{d}{dt}\left[\frac{1}{\sqrt{t}} \int_z^\infty \exp[-(\bar{x} - x)^2/4Lt]\, dx\right]\right\}$$

and since $\bar{x} = Ft/\xi a$,

$$\frac{dC}{dt} = \frac{-C_0}{\sqrt{4\pi L}}\left\{\frac{d}{dt}\left[\frac{1}{\sqrt{t}} \int_z^\infty \exp[-(Ft/\xi a - x)^2/4Lt]\, dx\right]\right\}$$

$$= \frac{-C_0}{\sqrt{4\pi L}} \int_z^\infty \left[\frac{-1}{2\sqrt{t^3}} \exp[-(Ft/\xi a - x)^2/4Lt] + \frac{2F}{\xi a\sqrt{t}} \frac{(Ft/\xi a - x)}{4Lt} \exp[-(Ft/\xi a - x)^2/4Lt]\right.$$

$$\left. + \frac{(Ft/\xi a - x)^2}{\sqrt{t}\, 4t^2 L} \exp[-(Ft/\xi a - x)^2/4Lt]\right] dx.$$

Assume that $Ft/\xi a - x$ remains finite as t becomes large then the third term in the sum becomes small compared to the others. Also assume dC/dt can be approximated by $\Delta C/\Delta t$ (a major problem). Then

$$\Delta C(x) = \frac{-C_0 \Delta t}{\sqrt{4\pi L}} \int_z^\infty \left[-\frac{1}{2\sqrt{t^3}} \exp[-(Ft/\xi a - x)/4Lt] + \frac{2F}{\sqrt{t}} \frac{(Ft/\xi a - x)}{\xi a 4Lt} \exp[-(Ft/\xi a - x)^2/4Lt]\, dx\right]$$

Let $Q = (Ft/\xi a - x)^2/4Lt$, then $dQ = (-2/4Lt)(Ft/\xi a - x)dx$. Thus

$$\Delta C(x) = \frac{-C_0 \Delta t}{\sqrt{4\pi L}} \int_{z'}^\infty \left[\frac{Lt}{\sqrt{t^3}(Ft/\xi a - x)} e^{-Q} - \frac{F}{\xi a\sqrt{t}} e^{-Q}\right] dQ$$

$$= \frac{C_0 \Delta t}{\sqrt{4\pi L}}\left[\int_{z'}^\infty -\frac{\sqrt{Lt}}{2\sqrt{Qt^3}} e^{-Q} dQ + \int_{z'}^\infty \frac{F}{\xi a\sqrt{t}} e^{-Q} dQ\right].$$

The first term, $(-C_0 \Delta t/\sqrt{4\pi L}) \int_{z'}^\infty (\sqrt{Lt}/2\sqrt{Qt^3}) e^{-Q} dQ$ is of the form $A \int_{z'}^\infty (e^{aY}/y^m) dy$, where $a = -1$, $m = \frac{1}{2}$ and $A = -C_0 \Delta t \sqrt{Lt}/2\sqrt{4\pi L t^3}$. Thus

$$\int_{z'}^{\infty} \frac{e^{ay}}{y^m}\,dy = -\frac{1}{m-1}\,\frac{e^{ay}}{y^{m-1}} + \frac{a}{m-1}\int_{z'}^{\infty} \frac{e^{ay}}{y^{m-1}}\,dy$$

and can be expanded indefinitely.

Putting values for m and a one obtains

$$\int_{z'}^{\infty} \frac{e^{-y}}{\sqrt{y}}\,dy = 2e^{-y}\left[\sqrt{y} + \frac{2\sqrt{y^3}}{3} + \frac{4\sqrt{y^5}}{15} + \frac{8\sqrt{y^7}}{105} + \ldots\right]\Bigg|_{z'}^{\infty}.$$

At the upper limit, where $y = \infty$, the terms in the expression are all of the form $0 \cdot \infty$ but repeated applications of l'Hospital's rule show that all terms equal 0. At the lower limit, $z' = Q = (\bar{x} - x)^2/4Lt$, so if we assume that terms above the third term drop out

$$A\int_{z'}^{\infty} \frac{e^{-Q}}{\sqrt{Q}}\,dQ = \frac{(\bar{x} - x)C_0\Delta t}{4t\sqrt{\pi Lt}}\exp[-(\bar{x} - x)^2/4Lt] + \frac{C_0\Delta t(\bar{x} - x)^3}{24t^2L\sqrt{\pi Lt}}\exp[-(\bar{x} - x)^2/4Lt]$$

$$= \tfrac{1}{4}\frac{(\bar{x} - x)C_0\Delta t}{t\sqrt{\pi Lt}}\left[1 + \tfrac{1}{6}\frac{(\bar{x} - x)^2}{Lt}\right]\exp[-(\bar{x} - x)^2/4Lt],$$

or for convenience

$$B(\bar{x} - x)e^{-Q} + D(\bar{x} - x)^3e^{-Q}.$$

The second term in the $\Delta C(x)$ equation, $(C_0\Delta t/\sqrt{4\pi L})\int_{z'}^{\infty}(F/\xi a\sqrt{t})e^{-Q}\,dQ$ is

$$-\frac{C_0\Delta t}{\sqrt{4\pi Lt}}\,\frac{F}{\xi a}\,e^{-Q}\Big|_{z'}^{\infty} = \frac{C_0\Delta t}{\sqrt{4\pi Lt}}\,\frac{F}{\xi a}\exp[-(\bar{x} - x)^2/4Lt].$$

Thus $\Delta C(x) = B(\bar{x} - x)e^{-Q} + D(\bar{x} - x)^3e^{-Q} + (C_0\Delta t F/\xi a\sqrt{4\pi Lt})e^{-Q}$.

The second moment, l^2, defined by Chun is $l^2 = \int_{-\infty}^{\infty}\Delta C(x)(\bar{x} - x)^2\,dx$; remembering $\phi = (\bar{x} - x)$ and $d\phi = -dx$, this gives

$$l^2 = -\int_{-\infty}^{\infty} B\phi^3\exp(-\phi^2/4Lt)\,d\phi - \int_{-\infty}^{\infty} D\phi^5\exp(-\phi^2)\,d\phi - \int_{-\infty}^{\infty}\frac{C_0\Delta t}{\xi a\sqrt{4\pi Lt}}\exp(-\phi^2/4Lt)\,d\phi.$$

But

$$\int_{-\infty}^{\infty}\phi^3\exp(-\phi^2/4Lt)\,d\phi = 0; \qquad \left[\int_0^{\infty} y^3e^{-ay^2}\,dy = \frac{\sqrt{\pi}}{2a^{3/2}} = -\int_{-\infty}^{0} y^3e^{-ay^2}\,dy\right]$$

and

$$\int_{-\infty}^{\infty}\phi^5\exp(-\phi^2/4Lt)\,d\phi = 0; \quad \left[\int_0^{\infty} y^5e^{-ay^2}\,dy = \frac{1}{a^3} = -\int_{-\infty}^{0} y^5e^{-ay^2}\,dy\right].$$

But

$$-\frac{C_0 \Delta t F}{\xi a \sqrt{4\pi L t}} \int_{-\infty}^{\infty} e^{-\phi} d\phi = \frac{2C_0 \Delta t F t L}{\xi a}; \qquad \left[\int_{-\infty}^{\infty} y^2 e^{-ay^2} dy = \frac{\sqrt{\pi}}{2a^{3/2}}, \quad a = \frac{1}{4Lt} \right].$$

Since $Ft/\xi a = \bar{x}$,

$$l^2 = 2C_0 \Delta t \bar{x} L.$$

Remembering that the C_0 measured by the scanning gel chromatograph is $C_0' = \xi C_0$

$$L = l^2 / 2\xi C_0 \Delta t \bar{x}.$$

References

[1] E.E. Brumbaugh and G.K. Ackers, J. Biol. Chem. 243 (1968) 6315.
[2] H.W. Warshaw and G.K. Akers, Anal. Biochem. 42 (1971) 405.
[3] G.K. Ackers, E.E. Brumbaugh, S.C.H. Ip and H.R. Halvorson, Biophys. Chem. 4 (1976) 171.
[4] H.R. Halvorson and G.K. Ackers, J. Poly. Sci. A-2 9 (1971) 245.
[5] H.R. Halvorson and G.K. Ackers, J. Biol. Chem. 249 (1974) 967.
[6] R. Valdes, Jr., L.P. Vickers, H.R. Halvorson and G.K. Ackers, Proc. Natl. Acad. Sci. USA 75 (1978) 5493.
[7] L.P. Vickers and G.K. Ackers, Biophys. Chem. 7 (1977) 299.
[8] E.E. Brumbaugh and G.K. Ackers, Anal. Biochem. 41 (1971) 543.
[9] M.M. Jones, G.A. Harvey and G.K. Ackers, Biophys. Chem. 5 (1976) 339.
[10] G.K. Ackers, Methods of Protein Separation 2 (1976) 1.
[11] E.E. Saffen, E.E. Brumbaugh and P.W. Chun, Fed. Proc. 37 (1978) 1710.
[12] E.E. Brumbaugh, E.E. Saffen and P.W. Chun, Biophys. Chem. 9 (1979) 299.
[13] E.E. Saffen and P.W. Chun, Biophys. Chem. 9 (1979) 329.
[14] J.K. Zimmerman, D.J. Cox, and G.K. Ackers, J. Biol. Chem. 246 (1971) 4242.
[15] J.K. Zimmerman and G.K. Ackers, J. Biol. Chem. 246 (1971) 1078.
[16] D.J. Cox, Arch. Biochem. Biophys. 112 (1965) 249.
[17] D.J. Cox, Arch. Biochem. Biophys. 112 (1965) 259.
[18] D.J. Cox, Arch. Biochem. Biophys. 119 (1976) 230.
[19] D.J. Cox, Arch. Biochem. Biophys. 129 (1969) 106.
[20] G.K. Ackers, Adv. Prot. Chem. 24 (1970) 343.
[21] G.K. Ackers, The Proteins 1 (1975) 1.